DOI: 10.1002/ejic.200600030

# Water-Soluble $Sal_2en$- and Reduced $Sal_2en$-Type Ligands: Study of Their $Cu^{II}$ and $Ni^{II}$ Complexes in the Solid State and in Solution

**Isabel Correia,[a] Agnes Dornyei,[b] Tamás Jakusch,[c] Fernando Avecilla,[d] Tamás Kiss,*[b,c] and João Costa Pessoa*[a]**

**Keywords:** Copper(II) / Nickel(II) / Reduced Schiff bases / Speciation / Crystal structure

The $Cu^{II}$ and $Ni^{II}$ complexes of the Schiff base $pyr_2en$ [*N*,*N*′-ethylenebis(pyridoxyliminato)] and reduced Schiff bases $Rpyr_2en$ [*N*,*N*′-ethylenebis(pyridoxylaminato)] and $R(SO_3$–sal$)_2en$ ($SO_3$–sal = salicylaldehyde-5-sulfonate) were prepared and characterized by elemental analysis, IR, UV/Vis, and EPR spectroscopy. The structure of $Ni(pyr_2en)\cdot 3H_2O$ was determined by single-crystal X-ray diffraction. The $pyr_2en^{2-}$ ligand is coordinated through two phenolate-O and imine-N atoms, in a distorted square-planar geometry. The complexation of $Cu^{II}$ and $Ni^{II}$ with $Rpyr_2en$ in aqueous solution is studied by pH-potentiometry, UV/Vis spectroscopy, as well as by EPR spectroscopy for the $Cu^{II}$ system, and $^1H$ NMR spectroscopy for the $Ni^{II}$ system. Complex formation constants were determined and binding modes proposed. While for the $Cu^{II}$ system all complexes present a 1:1 stoichiometry with different protonation states, for the $Ni^{II}$ system the 2:1 (L/M) complexes become important in the basic pH range at a higher ligand excess.


## Introduction

The application of Green Chemistry principles in organic transformations has attracted increased attention in the development of transition metal catalysts. $Sal_2en$-type ligands derived from *o*-hydroxyaldehydes and diamines are one of the most important ligand systems in asymmetric, homogeneous, and heterogeneous catalysis and in stereoselective synthesis.[1–5] Their transition metal complexes can be used in a large variety of applications, namely asymmetric ring opening of epoxides,[4] cyclopropanation,[6] and enantioselective epoxidation of olefins.[7] Their versatility and selectivity in chemical reactions is partly due to the ability of $sal_2en$-type ligands to complex a variety of transition metals in several oxidation states. They normally form square-pyramidal or octahedral complexes in which the four donor atoms coordinate in an almost planar fashion. Numerous $sal_2en$-type ligands have been synthesized and investigated, but most of them show low solubility in aqueous solution, which can be overcome by changing the diamine precursor and/or the ring substituents on the aldehyde.

In solution, Schiff base (SB) ligands have the disadvantage of the hydrolysis of the C=N bond, particularly in water-containing solvents. Reduction of the SB to give an amine may present interesting advantages. The reduced SBs (hereafter designated by $sal_2an$) are not so prone to hydrolysis and are more flexible and unrestrained to remain planar when coordinated to a metal center. Several $sal_2an$ complexes have been synthesized and characterized, namely with $Cu^{II}$,[8–10] $Co^{II}$,[8] $Ni^{II}$,[11] $VO^{IV}$,[12,13] $Fe^{III}$,[14] and $Zn^{II}$.[15] In the $Ni^{II}$ and $Co^{II}$ complexes the ligand coordinates in a slightly distorted square-planar geometry, and these complexes have shown the ability to interact with oxygen:[9,11] when dissolved in organic solvents these complexes can undergo oxidative dehydrogenation,[9,11] i.e. in the presence of $O_2$ one of the C–N bonds may be oxidized to an imine-type bond. This process has not been observed in most of the $Cu^{II}$ complexes, which are stable in organic solutions exposed to air.

One of the guidelines in Green Chemistry research is the elimination of hazardous solvents in reaction media. As mentioned above, $sal_2en$ complexes are frequently used as catalysts for several applications. As most $sal_2en$ complexes are not water soluble one of our objectives is the synthesis of water-soluble ligands and complexes.

In a previous work[12] we reported the preparation and characterization of the Schiff base *N*,*N*′-ethylenebis(pyridoxyliminato) ($pyr_2en$) and its reduced derivative *N*,*N*′-ethylenebis(pyridoxylaminato) ($Rpyr_2en$). Their $V^{IV}O$ and $V^{V}O_2$ complexes were characterized in the solid state and in

[a] Centro Química Estrutural, Instituto Superior Técnico, Av. Rovisco Pais, 1049-001 Lisboa, Portugal
[b] Department of Inorganic and Analytical Chemistry, University of Szeged, P. O. Box 440, 6701 Szeged, Hungary
[c] Bioinorganic Chemistry Research Group of the Hungarian Academy of Sciences, Department of Inorganic and Analytical Chemistry, University of Szeged, P. O. Box 440, 6701 Szeged, Hungary
[d] Departamento de Química Fundamental, Universidade da Coruña, Campus de A Zapateira, 15071 A Coruña, Spain
Supporting information for this article is available on the WWW under http://www.eurjic.org or from the author.

  

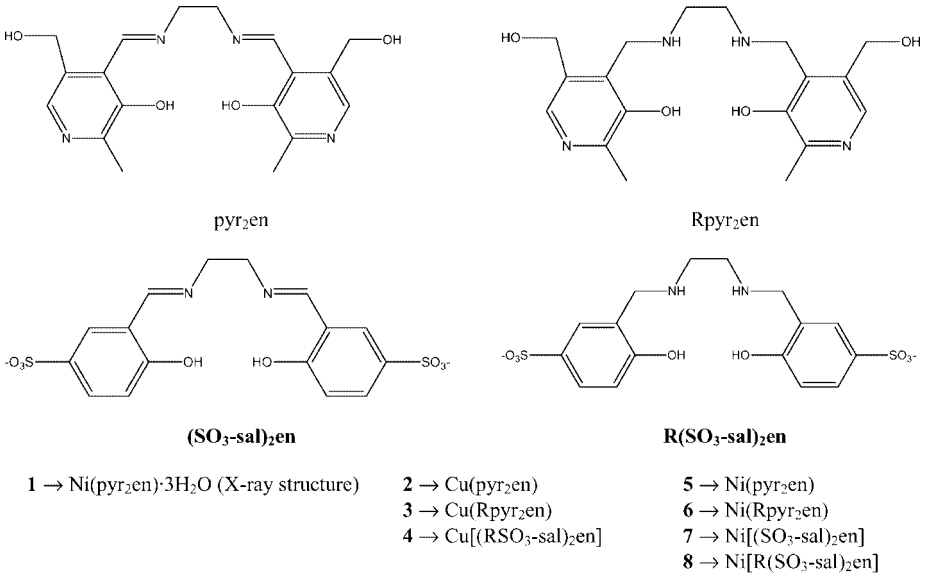


**1** → Ni(pyr$_2$en)·3H$_2$O (X-ray structure)
**2** → Cu(pyr$_2$en)
**3** → Cu(Rpyr$_2$en)
**4** → Cu[(RSO$_3$-sal)$_2$en]
**5** → Ni(pyr$_2$en)
**6** → Ni(Rpyr$_2$en)
**7** → Ni[(SO$_3$-sal)$_2$en]
**8** → Ni[R(SO$_3$-sal)$_2$en]

Scheme 1. Structural formulae of the prepared complexes. The complex characterized by single-crystal X-ray diffraction is indictaed.

solution. The molecular structure of two dioxovanadium(V) complexes with this reduced SB evidenced the tetradentate binding mode and the flexibility of the Rpyr$_2$en when coordinated to the metal ion. The solution studies showed that Rpyr$_2$en forms much more stable complexes with $V^{IV}$ and $V^{V}$ than the corresponding Schiff base pyr$_2$en, and that the SB has a much higher tendency to hydrolyze in aqueous solution. This is reflected in the proton displacement constants ($K$*), characteristic for the formation equilibrium: $H_6L + V^{IV}O^{2+} \leftrightarrows [V^{IV}OLH_2]^{2+} + 4H^+$; the log$K$* values are –14.1 and –5.63 for pyr$_2$en and Rpyr$_2$en, respectively.[12] Similar results were obtained for (SO$_3$–sal)$_2$en and R(SO$_3$–sal)$_2$en with their vanadium complexes.[16]

In this work we report on the preparation of several new moderately water-soluble $Cu^{II}$ and $Ni^{II}$ complexes (the ligands and formula names are shown in Scheme 1), one of them characterized by single-crystal X-ray diffraction. We also report on the solution study of the reduced SB Rpyr$_2$en with $Cu^{II}$ and $Ni^{II}$ by pH-potentiometry, visible absorption (Vis), EPR ($Cu^{II}$), and $^1$H NMR ($Ni^{II}$) spectroscopy.

## Results and Discussion

### Synthesis and Characterization of the Solid Compounds

Sal$_2$en-type ligands were prepared by the condensation of ethylenediamine with the aldehyde derivative. Reduction with NaBH$_4$ yielded the reduced SB.[12,16] From solutions containing $Ni^{II}$ and Rpyr$_2$en, orange crystals of the SB complex Ni(pyr$_2$en)·3H$_2$O were obtained. This implies that the two amine bonds underwent dehydrogenation. The solid-state characterization of all complexes was done by taking into account that this process might also have occurred with the other metal complexes. For the Rpyr$_2$en complexes the characterization (elemental analysis, IR, and UV/Vis spectroscopy) is consistent with a formulation of M(Rpyr$_2$en) (M = $Ni^{II}$ or $Cu^{II}$). Complex K$_2${Ni[R(SO$_3$–sal)$_2$en]}, although it was characterized and is included here, is not stable; its color changes from grey, immediately after the synthesis, to soft pink, and after a week to brown. The ESI mass spectrum, measured for solutions of the pink solid, confirms the presence of the reduced Schiff base showing important peaks that can be assigned to [NiL + 2K + 1]$^+$ ($m/z$ = 565) and [NiL + 3K]$^+$ ($m/z$ = 603).

### X-ray Diffraction Studies

#### *Ni(pyr$_2$en)·3H$_2$O (1)*

Figure 1 includes an ORTEP representation of the molecular structure of Ni(pyr$_2$en)·3H$_2$O (**1**), and Table 1 shows selected bond lengths and angles. The molecule is neutral with both pyridinic nitrogens deprotonated, and the ligand coordinates the Ni atom through two phenolate oxygen ($O_{phenolate}$) and two imine nitrogen ($N_{imine}$) atoms. The geometry around the metal ion is distorted square planar, and there are three water molecules in the asymmetric unit (not shown). The planar arrangement Ni(ONNO) is slightly distorted due to the *cis*/*trans* angles, which are not 90° and 180°. The *cis* and *trans* angles are 84.2 and 94.8°, and 178.4 and 178.5°, respectively. The ligand forms a set of chelate rings of (6+5+6)-members, and the highest deviation from planarity is found in the ring defined by Ni(1)–N(1)–C(2)–C(1)–N(2), which has an rms value of 0.1074(75) Å (the others are less than 0.05 Å). It is noteworthy that the torsion angle between the N(1)–C(2)–C(1)–N(2) atoms is only 29.24(1.71)°, lower than those previously observed in this type of complexes.[17] The pyridoxal rings are planar, with rms values of 0.0172(63) and 0.0127(58) Å.

The Ni–O and Ni–N bond lengths are similar and in the usual range found for $Ni^{II}$–sal$_2$en-type complexes.[11,18–21] The C–O distances are also typical for this type of ligands,[9,11,19–21] and the C=N bonds show double bond character with distances of ca. 1.3 Å. After coordination to

  

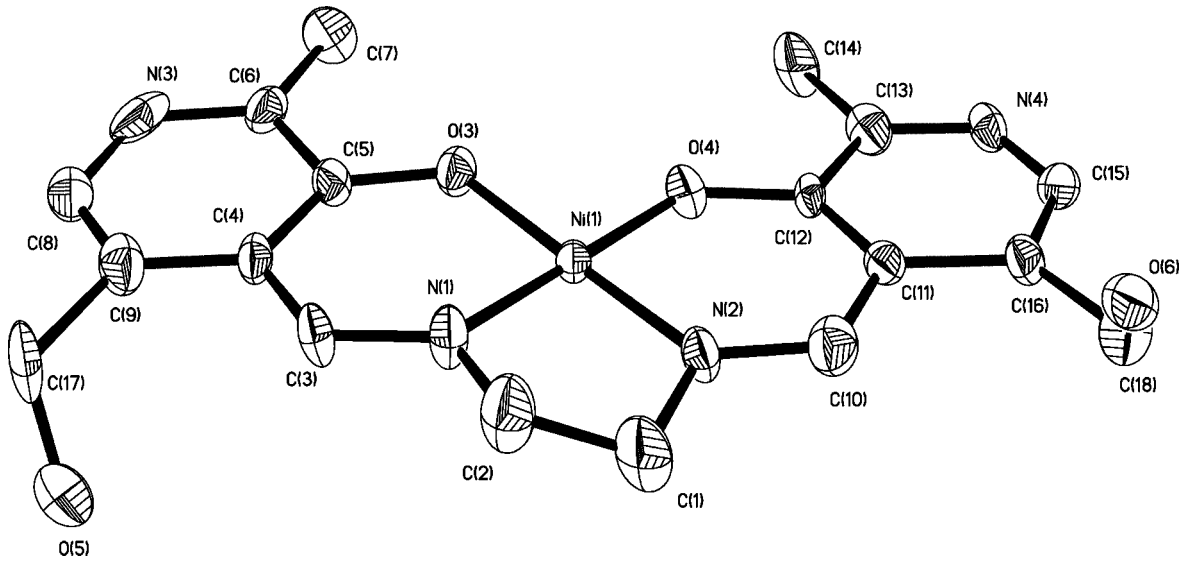


Figure 1. ORTEP diagram of $Ni(pyr_2en)\cdot 3H_2O$ (**1**) showing the atom labeling scheme. The thermal ellipsoids were drawn at the 30% probability level. The water molecules were omitted for clarity.

Table 1. Selected bond lengths [Å] and angles [°] for complex $Ni(pyr_2en)\cdot 3H_2O$ (**1**).

| Bond lengths [Å] | | Bond angles [°] | |
|---|---|---|---|
| Ni(1)–O(3) | 1.838(5) | O(3)–Ni(1)–O(4) | 84.2(3) |
| Ni(1)–O(4) | 1.842(5) | O(3)–Ni(1)–N(1) | 94.4(3) |
| Ni(1)–N(1) | 1.849(7) | O(4)–Ni(1)–N(1) | 178.5(3) |
| Ni(1)–N(2) | 1.821(7) | O(3)–Ni(1)–N(2) | 178.4(3) |
| O(3)–C(5) | 1.310(10) | O(4)–Ni(1)–N(2) | 94.8(3) |
| O(4)–C(12) | 1.328(9) | N(1)–Ni(1)–N(2) | 86.7(3) |
| N(2)–C(1) | 1.455(12) | | |
| N(2)–C(10) | 1.308(11) | | |
| N(1)–C(2) | 1.451(12) | | |
| N(1)–C(3) | 1.262(10) | | |

the metal ion the ligand does not undergo a significant change in the $C–O_{phenolic}$ and $C–N_{imine}$ bond lengths: the C–O bonds decrease by 0.034 Å and the C=N bonds increase by 0.035 Å.[12] In the complex the $HO–(CH_2)–$ groups of the pyridoxal rings are perpendicular to the apparent molecular plane, in an *anti* position to each other. This results in a three-dimensional crystalline structure connected by H bonds. ESI-1 shows the crystalline packing and emphasizes the intermolecular bonds. The molecular planes are approximately parallel, but overlaid in an alternate manner; this is probably because of the *anti* position of the hydroxy groups. The distance between neighboring Ni atoms is between 6.381 and 8.268 Å.

### Infrared Spectroscopy

Table 2 contains selected IR bands of the complexes. The assignment was based on data from refs.[22–25] and by comparison with the spectra of the ligands.[12] All complexes present broad bands in the 2400–3600 $cm^{-1}$ range, which correspond to the stretching vibration (symmetric and antisymmetric) of the $CH_2O–H$ groups of the pyridoxal rings (for the $Rpyr_2en$ complexes) and to the water molecules. The weak $\nu$(N–H) band that emerged from the broad band at 3286 $cm^{-1}$ in $Rpyr_2en$[12] appears in the complexes at lower wavenumbers, in agreement with the coordination through the $N_{amine}$ groups. The $\nu(C–O)_{phenolate}$ band appears in the normal range for these types of complexes.[23,26] The strong $\nu$(C=N) band of complex $Cu(pyr_2en)$ is assigned to the band at 1635 $cm^{-1}$, at a higher wavenumber than the ligand (1626 $cm^{-1}$),[12] and no such band is seen in the IR spectrum of $Cu(Rpyr_2en)$. Similarly, while the $\nu$(C=N) band of $Ni(pyr_2en)$ appears at ca. 1620 $cm^{-1}$, no band is seen in the IR spectrum of $Ni(Rpyr_2en)$, which might be assigned to this vibration. Complex $Ni[(SO_3–sal)_2en]$ presents a very

Table 2. Selected IR [$cm^{-1}$] and UV/Vis absorption bands of the prepared complexes.

| | FT-IR $\nu(N–H)_{stretch}$ | $\nu$(C=N) | $\nu(C–O)_{phenolate}$ | $\nu$(O–H) | UV/Vis Solvent | $\lambda_{max}$ [nm] ($\varepsilon$ [$M^{-1}\,cm^{-1}$]) |
|---|---|---|---|---|---|---|
| **1** | – | 1618 (s) | 1197 (m) | broad band at 3600–2900 | DMSO | 360 (8000), 426 (5000) |
| **2** | – | 1635 (s) | 1207 (m) | broad band centered at 3400 | DMSO | 260 sh (9100), 280 (11800), 380 (10000), 580 (345) |
| **3** | 3285 (w) | – | 1244 (m) | broad band at 3600–2900 | DMSO | 260 (10000), 310 (11000), 355 sh (1660), 625 (318) |
| **4** | several bands | – | 1182 (s) | broad band at 3600–2900 | $H_2O$ | 420 sh (260), 635 (83) |
| **5** | – | 1620 (s) | 1204 (s) | broad band at 3600–2800 | DMSO | 265 (24000), 275 sh (21750), 360 (8500), 427 (5300) |
| **6** | 3385 (w) | – | 1250 (m) | broad band at 3600–2800 | DMSO | 263 (27300), 315 (10500), 495 (542) |
| **7** | – | 1609 (s) | 1204 (s) | broad band centered at 3350 | $H_2O$ | 296 sh (7500), 384 (4600), 416 sh (2500) 508 sh (150) |
| **8** | 3271 (w, br) | – | 1185 (s) | broad band at 3600–2900 | $H_2O$ | 254 (18700), 328 sh (557), 378 sh (325), 450 sh (77) |

  

strong band at 1609 $cm^{-1}$ assigned to $\nu$(C=N). This band is absent in the corresponding reduced SB complex Ni[R($SO_3$–sal)$_2$en], which presents bands at 1593 and 1639 $cm^{-1}$, assigned to aromatic =C–H and C=C stretching vibrations.

### UV/Vis Absorption Spectroscopy

The UV/Vis spectra were recorded over the 250–900 nm range in DMSO or water. The results are summarized in Table 2. Some of the intense bands at low wavelengths ($\lambda <$ 400 nm) are assigned to charge transfer (CT), imine π-π* (when appropriate), and intramolecular transitions in the aromatic rings. In the visible range ($\lambda >$ 420 nm) the bands are predominantly due to d-d transitions. The copper complexes **2**–**4** have one well-defined broad d-d band at $\lambda_{max}$ = 550–650 nm, and stronger bands at ca. $\lambda$ = 380–420 nm from the $Cu^{II} \rightarrow$ phenolate (π*) transitions [and also imine π-π* in the case of Cu(pyr$_2$en)], which is in agreement with that expected for tetrahedrally distorted square-planar complexes of the $CuO_2N_2$ type.[27,28] The $Ni^{II}$ complexes **5**–**8** have low intensity broad bands in the 400–550 nm range, assigned to transitions from the four low-lying d orbitals to the σ antibonding $d_{x^2-y^2}$ orbital. At higher energies ($\lambda <$ 400 nm) a group of high intensity bands appears, and in the case of Ni(pyr$_2$en) and Ni[($SO_3$–sal)$_2$en] relatively intense bands from the imine π-π* transition also show up. The UV/Vis data of the complexes in DMSO are in agreement with that expected for $Ni^{II}$ and $Cu^{II}$ complexes with square-planar geometries.[9,10,27] The relatively high $\varepsilon$ values of the d-d bands of the Ni complexes suggest some borrowing of intensity from CT bands and/or a significant distortion of the coordination geometry.

### EPR Spectroscopy

The EPR spectra of the $Cu^{II}$ complexes were measured in "frozen" ($T \approx$ 77 K) solutions of an adequate solvent. The spectrum of Cu(pyr$_2$en) in DMSO showed a broad band centered at $g$ = 1.995 without hyperfine structure. This is probably because of molecular aggregation during the freezing process. No signal was detected at $g$ = 4.

The EPR spectrum of Cu(Rpyr$_2$en) was measured in water and DMSO at 77 K. Both show well-resolved hyperfine structure and suggest axial symmetry. The spin Hamiltonian parameters were obtained by computer simulation of the experimental spectra using a program from Rockenbauer and Korecz.[29] Among other factors, the $g_\parallel$ and $A_\parallel$ values depend on the nature of the donor atoms and can be used to confirm the binding mode. The parameters (DMSO: $g_\perp$ = 2.047, $A_\perp = 22.2\times10^{-4}$ $cm^{-1}$, $g_\parallel$ = 2.233, $A_\parallel = 197.3\times10^{-4}$ $cm^{-1}$; $H_2O$: $g_\perp$ = 2.052, $A_\perp = 38.4\times10^{-4}$ $cm^{-1}$, $g_\parallel$ = 2.237, $A_\parallel = 193.5\times10^{-4}$ $cm^{-1}$) fit well with that expected for a $N_2O_2$ binding mode.[30] On the other hand, the $g_\parallel/A_\parallel$ ratio of 113 in DMSO and 116 in $H_2O$ indicates a square-planar coordination environment.[30] In the spectrum of Cu(Rpyr$_2$en), dissolved in water, superhyperfine structure is observed in the perpendicular region of the spectrum, arising from the interaction of the $Cu^{II}$ unpaired electron with the two nitrogen donor atoms of the ligand, which results in a five line splitting ($A_N = 10.5\times10^{-4}$ $cm^{-1}$).

In the EPR spectrum of Cu[R($SO_3$–sal)$_2$en], dissolved in $H_2O$, more than one species is present. Observation of the low-field range and comparison with the EPR spectrum of $[Cu(OH_2)_6]^{2+}$ in the same solvent, shows that part of the ligand was removed from the coordination sphere of the metal ion upon dissolution and that some free $Cu^{2+}$ is present in solution (see ESI-2). Since the simulation of such $Cu^{II}$ spectra with more than one species is difficult, only an estimate of the parameters for the complex was obtained: $g_\parallel$ = 2.25 and $A_\parallel = 189\times10^{-4}$ $cm^{-1}$. The $g_\parallel/A_\parallel$ ratio (119) also indicates a square-planar geometry for this complex.[30] These parameters are similar to those obtained for other $Cu^{II}$–sal$_2$an complexes, which present square-planar geometry and a $N_2O_2$ coordination mode.[8]

### Study of the Oxidative Dehydrogenation Process of Ni(Rpyr$_2$en)

Some $Ni^{II}$ complexes with the sal$_2$an-type ligands are able to react with dissolved $O_2$.[9,11] In solutions of organic solvents the complexes undergo oxidative dehydrogenation, and one of the two C–N bonds dehydrogenates yielding a C=N bond. Further dehydrogenation of the second C–N bond has not been previously observed.[9,11] Since crystals of Ni(pyr$_2$en) (**1**) were obtained from the filtrate solution of the Ni(Rpyr$_2$en) synthesis, we might expect that in the present system the dehydrogenation is complete. To further investigate the process, complex Ni(Rpyr$_2$en) was dissolved in DMSO and air was bubbled through the stirred solution over a period of three days; the initial pink solution slowly became orange. Another identical solution was saturated with $N_2$; it also became progressively orange but at a much slower rate. The process was monitored by UV/Vis spectroscopy and Figure 2 shows the spectra recorded for both solutions. Initially there is an isosbestic point at ca. 510 nm, indicating the transformation of the reduced SB complex into another species, but it is quite clear that the final product is not Ni(pyr$_2$en) (its spectrum is included in the figure for comparison). The spectrum of the final product obtained in solution has similar features to those reported for $Ni^{II}$ complexes of half dehydrogenated complexes:[9,11] two new bands develop at 390 and 460 nm.

$^1$H NMR spectra of complexes Ni(Rpyr$_2$en) and Ni(pyr$_2$en) were measured in $(CD_3)_2SO$. The spectrum of Ni(pyr$_2$en) did not change over 24 hours, and all peaks could be easily assigned (see Experimental Section), while after 24 hours the spectrum of Ni(Rpyr$_2$en) showed features corresponding to two compounds [half dehydrogenated complex and Ni(Rpyr$_2$en)], indicating that the complex suffered partial dehydrogenation at only one of its amine bonds.

  

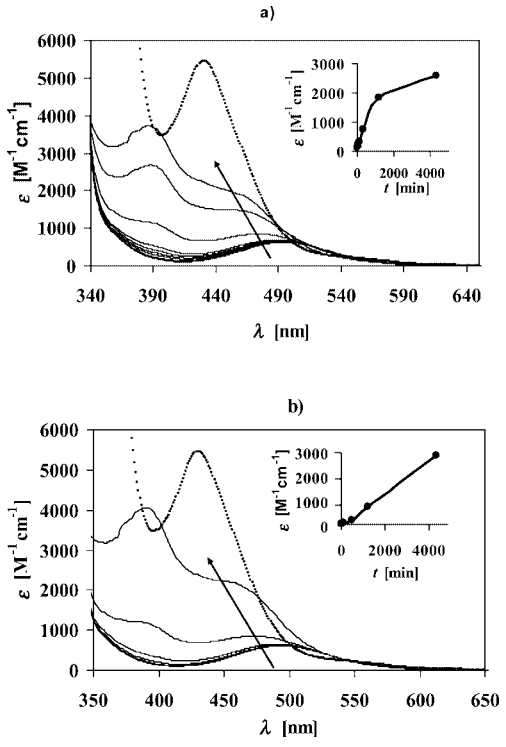


Figure 2. Time-dependence of the UV/Vis spectra of solutions containing Ni(R$pyr_2$en) in DMSO: (a) Bubbling air through the solution; (b) Under $N_2$ atmosphere. Insets: variation of the molar absorptivity at 412 nm. The arrows indicate increasing time (from 0 to 3 d). The spectrum of Ni($pyr_2$en) in DMSO (dotted) is included in both figures for comparison.

## Speciation Studies

The acid-base behavior of $pyr_2$en, R$pyr_2$en, and R($SO_3$–sal)$_2$en and their complexation with $V^{IV}$ and $V^{V}$ were previously reported.[12,16] The study of the $Cu^{II}$– and $Ni^{II}$–R$pyr_2$en systems by pH-potentiometry, Vis, EPR (for the $Cu^{II}$ system), and $^1$H NMR (for the $Ni^{II}$ system) spectroscopy is now presented.

### *$Cu^{II}$–R$pyr_2$en*

The pH-metric titration curves were measured between pH 2 and 11.3, and the best equilibrium model that fitted the experimental data corresponds to a model similar to that obtained for the $V^{IV}O$ system.[12] The stability constants are listed in Table 3 and a species distribution diagram is depicted in Figure 3 (a).

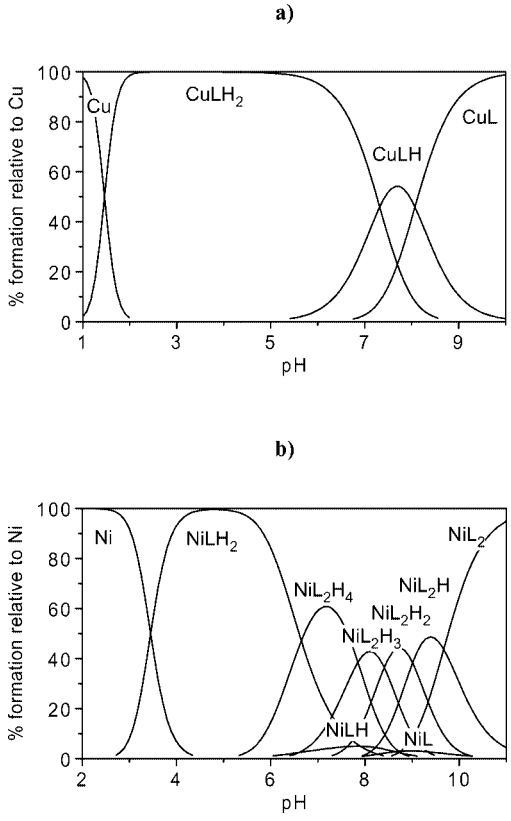


Figure 3. Species distribution diagram for the complexes formed in the (a) $Cu^{II}$–R$pyr_2$en system for solutions containing $C_{Cu}$ = 2.0 mmol dm$^{-3}$ and a L/M ratio of 2; (b) $Ni^{II}$–R$pyr_2$en system for solutions containing $C_{Ni}$ = 3.0 mmol dm$^{-3}$ and a L/M ratio of 4.

Analysis of the potentiometric data with the PSEQUAD program[31] shows the presence of only 1:1 complexes in solution over the whole pH range, in various protonation states. In the pH range 1–10 stoichiometries $[CuLH_2]^{2+}$, $[CuLH]^{+}$, and [CuL] are formed, with the deprotonations taking place at the N-pyridine atoms of the pyridoxal rings.

Table 3. Protonation and formation constants for the $M_pL_qH_r$ species formed in the $Cu^{II}$- and $Ni^{II}$-R$pyr_2$en systems, calculated from the pH-potentiometric and spectrophotometric data (EPR and UV/Vis) with the PSEQUAD program.[31]

| | $\log\beta_H$ (L = R$pyr_2en^{2-}$)[a] [12] | $\log\beta_H$[d] (L = pyrN$^-$) | | $\log\beta$ ($Cu^{II}$)[c] (L = R$pyr_2en^{2-}$) | $\log\beta$ ($Cu^{II}$)[d] (L = pyrN$^-$) | $\log\beta$ ($Ni^{II}$)[a] (L = R$pyr_2en^{2-}$) | $\log\beta$ ($Ni^{II}$)[d] (L = pyrN$^-$) |
|---|---|---|---|---|---|---|---|
| HL | 10.50 ± 0.01 | 10.41 | $MLH_2$ | 35.3 ± 0.3[c] | 21.34 | 28.52 ± 0.01 | – |
| $H_2L$ | 19.65 ± 0.01 | 18.56 | MLH | 28.04 ± 0.02 | 17.22 | 20.62 ± 0.02 | 14.20 |
| $H_3L$ | 27.33 ± 0.01 | 22.06 | ML | 19.98 ± 0.02 | 10.80 | 11.98 ± 0.02 | 6.46 |
| $H_4L$ | 33.30 ± 0.01 | | $ML_2H_4$ | – | – | 51.44 ± 0.03 | – |
| $H_5L$ | 36.31 ± 0.02 | | $ML_2H_3$ | – | 38.91 | 43.59 ± 0.04 | – |
| $H_6L$ | 38.60 ± 0.02 | | $ML_2H_2$ | – | 32.53 | 35.18 ± 0.04 | 28.14 |
| | | | $ML_2H$ | – | 25.46 | 26.17 ± 0.03 | – |
| | | | $ML_2$ | – | 17.47 | 16.50 ± 0.03 | 10.52 |
| | | | fitting[b] | $3.9 \times 10^{-3}$ [c] | | $3.0 \times 10^{-3}$ | |
| | | | no. of points | 244 | | 651 | |

[a] Three times the standard deviations (3×S.D.) of the calculations are included. [b] The average difference between the calculated and the experimental titration curves expressed in mL of titrant. The total initial volumes were 25 mL. [c] The S.D. values reflect the different calculated values from the pH-potentiometric and the spectroscopic data. [d] From ref.[32] ($I$ = 0.15 M $NaNO_3$; 37 °C).

  

The stability of the complexes is high, and even at pH 2 the amount of $[Cu(OH_2)_6]^{2+}$ is very small.

The Vis spectra for this system as the pH is varied (Figure 4) consists of a broad band (of d-d origin) with a maximum around 625 nm ($\varepsilon \approx 200$ mol dm$^{-3}$ cm$^{-1}$ at pH = 6.0). Deprotonation of the pyridine nitrogen atoms causes significant changes in the UV/Vis spectra: the d-d transition shifts to a higher energy as the pH is increased and the shoulder at ca. 420 nm (ascribed to phenolate → $Cu^{II}$ CT transition) shows a bathochromic effect with increasing pH. These shifts demonstrate that the pyridoxal ring forms a connected electron system and thus deprotonation of the pyridine-NH groups will influence the donor properties of the phenolate oxygen atoms.

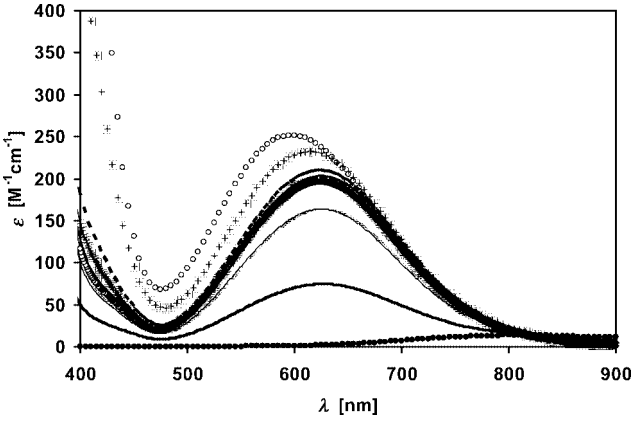


Figure 4. Visible spectra of aqueous solutions containing $Cu^{II}$ and $Rpyr_2en$, with $C_{Cu}$ = 5 mmol dm$^{-3}$ and a L/M ratio of 1 at several pH values. Below pH 2 the solutions were individually prepared and the $[H^+]$ was determined from a calibration curve (see Exp. Sect.). $[Cu(OH_2)_6]^{2+}$ (···), pH = 1.29 (——), 1.60 (——), 6.64 (---), 7.71 (+++), 10.56 (○). The superimposed spectra correspond to pH values in the pH range 2.2–6.0.

EPR spectra of samples containing $C_{Cu}$ = 5 mM and a L/M ratio of 1.1 at several pH values were measured at room temperature and 77 K. The parameters are collected in Table 4, and Figure 5 shows a few of the spectra obtained at room temperature. The frozen solution spectra (data not shown) show axial symmetry with resolved hyperfine structure, supporting the tetradentate binding of the ligand. For pH > 3 the spin Hamiltonian parameters do not show significant variation, confirming that the coordination mode for complexes $CuLH_2$, CuLH, and CuL is the same ($N_2O_2$),[30] that the deprotonation processes $[CuLH_2]^{2+} \rightarrow [CuLH]^+ \rightarrow [CuL]$ involve only the $NH^+_{pyridinic}$ groups of the ligand (these are not involved in the coordination), and that the coordination geometry is square planar.

It is clear from the speciation (Figure 3, a) and spectroscopic data (Figures 4 and 5) that for pH < 2 a significant amount of $Cu^{II}$ is already complexed by the ligand, and that the relevant data for calculation of the $\log\beta_{112}$ value occurs at pH ≤ 2. The visible absorption and room temperature EPR spectra were used to confirm the calculated stability constant obtained for $[CuLH_2]^{2+}$ and the proposed speciation model. The molar fraction of each species, obtained from both the EPR and visible absorption data for

Table 4. Spin Hamiltonian parameters for the $Cu^{II}$–$Rpyr_2en$ system obtained by computer simulation of the experimental spectra.[29]

| | $g_o$[a] | $A_o$ [×10$^4$cm$^{-1}$][a] | | |
|---|---|---|---|---|
| $[Cu(H_2O)_6]^{2+}$ | 2.196 | 32.7 | | |
| $CuLH_x$ [c] | 2.112 | 77.4 | | |
| | $g_\perp$[b] | $A_\perp$ [×10$^4$ cm$^{-1}$][b] | $g_\parallel$[b] | $A_\parallel$ [×10$^4$ cm$^{-1}$][b] |
| $[Cu(H_2O)_6]^{2+}$ | 2.082 | 1.8 | 2.417 | 133.1 |
| $CuLH_x$ [c] | 2.050 | 24.9 | 2.238 | 191.7 |

[a] Parameters obtained from spectra measured at room temperature. [b] Parameters obtained from spectra measured at 77 K (liquid nitrogen temperature). [c] $x$ = 0, 1, 2.

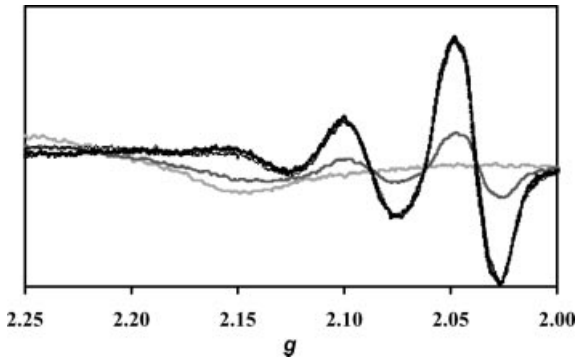


Figure 5. EPR X-band spectra (room temperature) of solutions containing $Cu^{II}$ and $Rpyr_2en$ with $C_{Cu}$ = 5 mmol dm$^{-3}$ and a L/M ratio of 1.1 at several pH values. $[Cu(OH_2)_6]^{2+}$ (light gray) and pH = 1.3 (dark gray). The superimposed black lines correspond to spectra measured at pH 1.6, 2.19 and 6.0.

pH ≤ 2 were introduced into the PSEQUAD program,[31] and a $\log\beta_{112}$ value of 35.64 ± 0.12 was refined for $CuLH_2$. On the other hand, from the pH-potentiometry data a $\log\beta_{112}$ = 35.01 ± 0.01 was obtained from data in the pH range 1.7–11, but varying the $\log\beta_{112}$ in the range 35.0–35.7 hardly affects the fitting parameter of the PSEQUAD program when using only the pH-metric data. The difference may be due to (i) the ionic strength, which was not exactly constant in the spectroscopic experiments at pH ≤ 2 and (ii) the higher error associated with the pH-metric data used in the pH range 1.7–2.0. The $\log\beta_{112}$ presented in Table 3 is the average of both values and the corresponding S.D. value reflects the different calculated values.

It should be emphasized that in complexes with the $sal_2an$ ligands, once each of the $N_{amine}$ atoms coordinates they become a stereogenic centers and *R* and *S* configurations become possible. Therefore, for each of the stoichiometries $MLH_2$, MLH, and ML at least three diastereoisomers are possible. These diastereoisomers are schematically represented by the configuration of the coordinated amine i.e. (*R*,*R*), (*S*,*S*), (*S*,*R*), or (*R*,*S*). Only for the MLH stoichiometry does the complex represented by (*S*,*R*) differ from (*R*,*S*). As found by DFT calculations for the $V^{IV}O$– and $V^{V}O_2$–$Rpyr_2en$ complexes,[12] the energies of the (*S*,*R*) and (*R*,*S*) diastereoisomers do not differ much from (*R*,*R*) or (*S*,*S*) (for this pair they are the same), and we predict that in solution all of them should form. With the techniques used

  

in this work it is not possible to distinguish between these different diastereoisomers.

Pyridoxamine (pyrN) is a vitamin $B_6$ analog and $Rpyr_2en$ can be seen as two pyridoxamine molecules linked by an ethylene bridge. The acid-base behavior and complexation of pyrN with $Cu^{II}$ and $Ni^{II}$ has been reported[32] and the data ($I$ = 0.15 M $NaNO_3$, 37 °C) is included in Table 3 for comparison. PyrN forms complexes with $Cu^{II}$ with the stoichiometry 1:1 and 2:1 (L/M) in various protonation states. The stability of the complexes formed in both ligand systems can be compared based on the constants ($\log K^*$) for the displacement of four protons: $H_6L + Cu^{2+} \leftrightarrows CuLH_2 + 4H^+$ (for $Rpyr_2en$), and $2H_3L + Cu^{2+} \leftrightarrows CuL_2H_2 + 4H^+$ (for pyrN). The $\log K^*$ values are –3.3 and –11.6, respectively. As expected, because of the chelate effect, the stability of the $Rpyr_2en$-$Cu^{II}$ complexes is much higher than that of the corresponding pyridoxamine complexes.

### *$Ni^{II}$–$Rpyr_2en$*

In equimolar solutions slow processes take place at pH > 8, and precipitation of a pink complex occurs. However, for solutions with L/M ratios greater than 1 the pH-metric titration curves could be measured up to 11.7. The model that best fitted the experimental data was obtained considering the formation of 1:1 and 2:1 complexes. Without bis complexes the fitting parameter of PSEQUAD was ca. five times higher. The stability constants obtained are listed in Table 3, and Figure 3b depicts a species distribution diagram.

As is usually the case for $Ni^{II}$ complexes the large zero-field splitting precluded the observation of any X-band resonances.[33] Although samples were measured by EPR spectroscopy, we were not able to obtain any EPR spectra. Moreover, $^1H$ NMR titrations carried out in $D_2O$ with L/M ratios of 1 and 4 confirmed that the $Ni^{II}$ complexes are paramagnetic. In fact, in solutions with a L/M ratio of 1, no $^1H$ NMR peaks were observed for pH > 3, where only metal bound ligand is present, while for pH < 3 only the peaks from the noncomplexed ligand are seen. In solutions with a L/M ratio of 4 only the free ligand peaks were observed, and for pH > 3 their areas decrease (when compared with the peak of the internal reference).

Spectroscopic data for solutions of complexes Cu($Rpyr_2en$) or Ni($Rpyr_2en$) in DMSO are consistent with a square-planar coordination of the $Rpyr_2en$ ligand. In water the spectroscopic data of Ni($Rpyr_2en$) is consistent with an octahedral geometry involving the donor set: $O_{phen}$, $N_{amine}$,$N_{amine}$,$O_{phen}$,$O_w$,$O_w$ ($O_{phen}$ = phenolate-$O^-$ donor atom, $N_{amine}$ = amine-N donor atom, $O_w$ = water-O atom).

In aqueous solutions containing $Ni^{II}$ and $Rpyr_2en$ the situation is more complex. To confirm the pH-metric results and the presence of the bis complexes, spectrophotometric measurements were carried out with L/M ratios of 1 and 4. Upon changing the pH the spectra show a continuous change, indicating that the speciation is much more complex than that for the $Cu^{II}$ system. Below pH 3 (Figure 6, a) the spectra present two d-d bands in the wavelength range shown, with maxima at ca. 725 and 395 nm, which can be assigned to the $[Ni(H_2O)_6]^{2+}$ transitions $^3T_{1g}(F) \leftarrow {}^3A_{2g}$ and $^3T_{1g}(P) \leftarrow {}^3A_{2g}$, respectively.[34] As the pH is increased stronger bands progressively build up. At pH 5.0, where species $NiLH_2$ is ca. 100% formed, the $\lambda_{max}$ are at 620 and 430 nm, and the latter transition [$^3T_{1g}(P) \leftarrow {}^3A_{2g}$, using the notation for an octahedral symmetry] overlapping the $O_{phen}$–Ni CT band tailing in from the UV region. Spectra were also measured for pH > 3 in the near IR range (see Supporting Information, Figure SI-7 in ESI-3), which show the presence of a broad band at ca. 995 nm ($\varepsilon$ = 18 mol dm$^{-3}$ cm$^{-1}$ at pH = 6.7), confirming the octahedral geometry of the complexes. This band, assigned to $^3T_{2g} \leftarrow {}^3A_{2g}$, gives a measure of the ligand field and shifts to higher energies between pH 3 and 6, confirming the increase in the field strength as the ligand replaces water in the $Ni^{II}$ coordination sphere. For solutions with a L/M ratio of 4 (Figure 6, b), the spectral features are the same as for L/M = 1 up to pH ca. 6, but above this pH the changes in the Vis spectra, upon increasing the pH, differ. With solutions containing L/M ratios of 4 no precipitation is observed below pH ca. 9.5, but at higher pH values a slight increase in the baseline suggests the presence of a small amount of precipitate. In the pH range 7.0–8.7, and for solutions with L/M = 4 (Figure 6, b), the spectra roughly intersect at 425 and 475 nm (not exactly isosbestic points) indicating the presence of two main types of species in equilibrium (between 1:1 and 2:1 complexes). Overall the Vis spectra confirm the species distribution diagram shown in Figure 3 (b).

ESI mass spectra were also measured to confirm the presence of the 2:1 (L/M) species. For aqueous solutions containing L/M = 1, $C_{Ni} \approx 1$ mM and pH = 5.3 several species were found in solution: $m/z$ = 363.5 $[L + 1]^+$, 419.3 $[NiL + 1]^+$, 455.0 $[NiL + 2H_2O]^+$, 781.0 $[NiL_2 + 1]^+$. For solutions containing L/M = 4, $C_{Ni} \approx 1$ mM and pH = 7.1: $m/z$ = 363.1 $[L + 1]^+$, 385.1 $[L + Na]^+$, 419.1 $[NiL + 1]^+$, 780.9 $[NiL_2 + 1]^+$. Although $NiL_2$ is found in both solutions, the intensity ratio of the MS peaks $NiL/NiL_2$ is 10:5 in the L/M = 1 solutions and 3.5:10 in the L/M = 4 solutions, showing the much higher importance of the bis complexes in solutions containing an excess of ligand.

$NiLH_2$ is the dominant species in the pH range 4–6 (see Figure 3). Its coordination geometry corresponds to a $O_{phen}$,$N_{amine}$,$N_{amine}$,$O_{phen}$,$O_w$,$O_w$ donor set, where the pyridine-N atoms are protonated. For pH > 5.5 the species $NiL_2H_4$, $NiL_2H_3$, $NiL_2H_2$, $NiL_2H$, and $NiL_2$ successively form up to a pH ca. 10.

For 2:1 complexes with tridentate ligands containing an $O_{phen}$, $N_{imine}$ or $N_{hydrazone}$, and $N_{amine}$ donor set binding modes corresponding to what is shown schematically as **I** have been characterized in the solid state by X-ray diffraction.[35–37] While in these compounds a significant part of each of the two ligands [($O_{phen}$ and $N_{imine}$ or $N_{hydrazone}$)] is constrained to be planar, the $Rpyr_2en$ ligand is much more flexible, and to the best of our knowledge this study is the first example of Ni–$sal_2en$- or Ni–$sal_2an$-type complexes reported showing the formation of bis complexes.

The intensity of the phenolate–$Ni^{II}$ CT band increases over the pH range ca. 5.3 to ca. 8.5. This suggests an in-

  

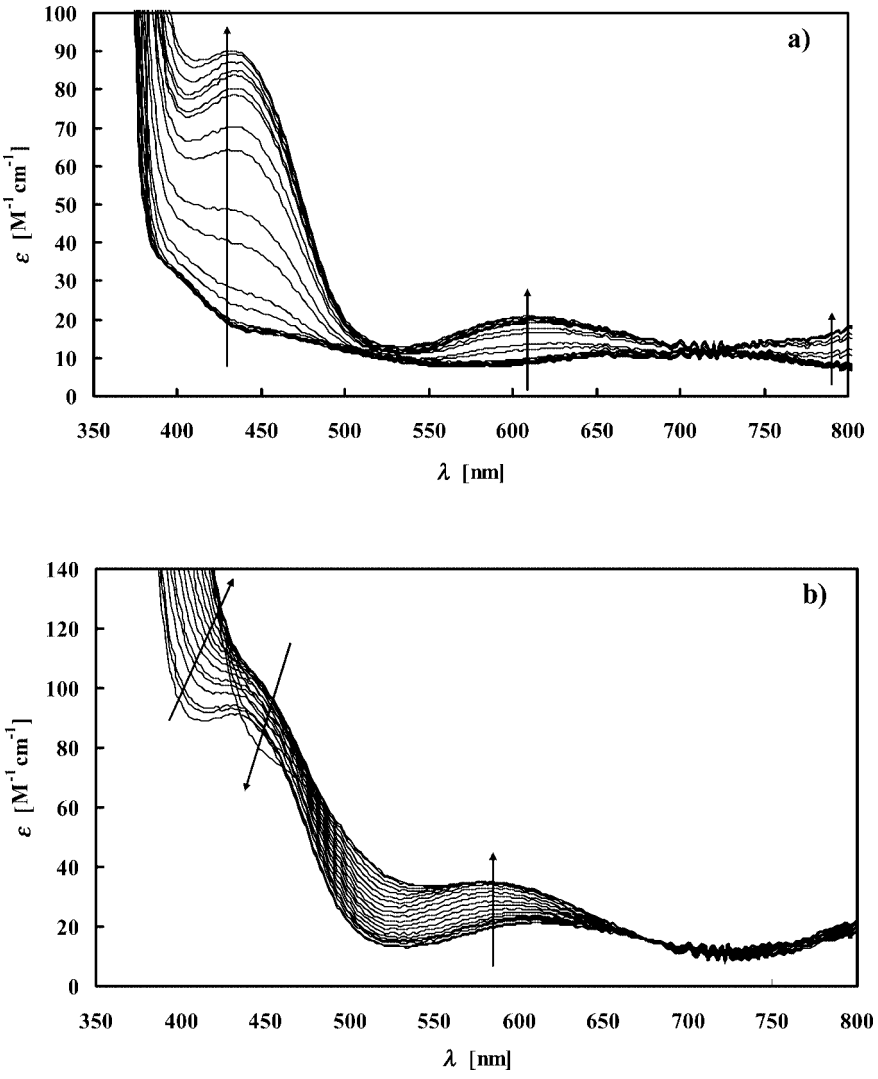


Figure 6. Visible spectra of aqueous solutions containing $Ni^{II}$ and $Rpyr_2en$, with $C_{Ni}$ = 2 mmol dm$^{-3}$ and L/M = 4 between (a) pH 2.10–5.02 and (b) pH 5.02–9.11. Arrows indicate increasing pH. Signal perturbations in the range 690–750 nm are due to instrumental noise.

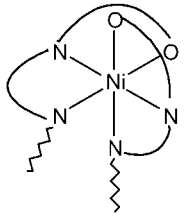


**I**

crease in the number of phenolate donor atoms in the $Ni^{II}$ coordination sphere upon the successive formation of $NiLH_2 \rightarrow NiL_2H_4 \rightarrow NiL_2H_3$. For pH > 8.7 the CT band remains approximately unchanged up to ca. 11.7, while the absorption over the wavelength range 450–800 nm increases until pH 10.3, and then decreases up to 11.7 (see Supporting Information, Figure SI-5 in ESI-3). However, the structure of the 2:1 Ni–$Rpyr_2en$ complexes in water is not easily anticipated. Formation of 2:1 complexes possibly involves displacement of one donor atom of the first ligand and the tridentate coordination of the second ligand. Binding modes such as **I** are a reasonable hypothesis, but the increase in intensity of the $O_{phen}$–Ni CT band may be indicative of the coordination of at least a third $O_{phen}$-donor atom.

The ratio $\log(K_{MLH_2}/K_{ML_2H_4}) = 0.55$ indicates a favorable interaction between the side chains in the bis complexes. These may be stabilized by intramolecular H bonds formed between groups of the coordinated ligands. In fact, the $Rpyr_2en$ ligand is quite flexible and contains several groups that may be involved in H bond formation: e.g. the pyridine-N atom (either as $N_{pyridine}$ or $NH^+_{pyridine}$), the –$(CH_2)$–OH groups of pyridoxal, or the phenolic-O atoms ($O_{phen}$ or $OH_{phen}$). Many possible binding modes and types of H bonds can be envisaged but discussing these further would be mainly speculation, as the techniques used do not help in this regard.

A comparison with pyridoxamine, which forms complexes of 1:1 and 2:1 L/M stoichiometry with $Ni^{II}$, can be

  

done based on the $\log K^*$ for the same equilibrium, as in the case of $Cu^{II}$ (see above); the $\log K^* = -10.08$ for $Rpyr_2en$ and –15.99 for pyrN[32] shows the higher stability of the $Rpyr_2en$ complexes, and also the lower stability of the $Ni^{II}$–$Rpyr_2en$ complexes when compared with those of $Cu^{II}$–$Rpyr_2en$.

## Conclusions

The coordination of the $sal_2en$- and $sal_2an$-type ligands $pyr_2en$, $Rpyr_2en$, and $R(SO_3–sal)_2en$ to $Cu^{II}$ and $Ni^{II}$ was investigated. These ligands form stable and moderately water-soluble complexes with $Cu^{II}$ and $Ni^{II}$. From solutions containing $Ni^{II}$ and $Rpyr_2en$, crystals of the SB complex $Ni(pyr_2en)$ were obtained, resulting from oxidative dehydrogenation of the two amine bonds, probably by molecular oxygen. The solution and solid-state characterization of the metal complexes showed that this process did not occur with the other complexes. Time-dependent visible absorption spectroscopic studies in aqueous solution with $Ni(Rpyr_2en)$ indicated that the dehydrogenation process, facilitated by molecular $O_2$, stops after oxidation of one amine bond. On standing for longer periods $Ni(pyr_2en)$ was obtained but only in the solid state.

The complexation of $Rpyr_2en$ with $Cu^{II}$ and $Ni^{II}$ could be studied by pH-potentiometry and spectroscopic techniques in aqueous solutions. In the $Cu^{II}$–$Rpyr_2en$ system very stable 1:1 complexes form, and at pH ca. 2 these correspond to ca. 95% of the total $Cu^{II}$. Characterization of the solid complex obtained indicates a square-planar coordination geometry involving the two $O_{phenolate}$ and two $N_{amine}$ as donor atoms. In the $Ni^{II}$–$Rpyr_2en$ system, when an excess of ligand is used bis complexes are formed in aqueous solution at pH > 6, avoiding the precipitation of the neutral NiL complex. The proton displacement constants ($K^*$) of the process $H_6L + M^{2+} \leftrightarrows ML{H_2}^{2+} + 4H^+$ are as follows: $K^*(CuLH_2^{2+}) = -3.27$; $K^*(V^{IV}OLH_2^{2+}) = -5.63$,[12] $K^*(NiLH_2^{2+}) = -10.08$, $K^*(ZnLH_2^{2+}) = -11.38$,[38] i.e. the stability order is $Cu^{II} > V^{IV}O > Ni^{II} > Zn^{II}$.

We should emphasize several aspects of the ligands studied in this work (or ligands obtained using the same aldehyde precursors and other diamines), which may have considerable advantages for e.g. catalytic applications using less toxic solvents, namely their higher solubility in aqueous and alcoholic solutions, when compared with most $sal_2en$-type ligands reported so far, because of the presence of hydrophilic groups in the aromatic rings. Moreover, the lower susceptibility to hydrolysis of the reduced $sal_2an$ derivatives, when compared with the corresponding SB, and the higher stability of $V^{IV}O$, $V^V$,[12] $Cu^{II}$, and $Ni^{II}$ complexes formed with the $sal_2an$-type ligands, may be important for both improving reaction yields and catalyst recovery. Finally, the higher flexibility of the $sal_2an$-type ligands and the fact that the coordinated $N_{amine}$ atoms are stereogenic centers may also prove useful for asymmetric synthesis if suitable diamine and/or aldehyde precursors are chosen. In the particular case of $Rpyr_2en$, with ligands containing $N_{pyridinic}$ atoms, the possibility of the various protonation states for the pyridinic nitrogens, which do not participate in coordination to the metal ions, allowing the formation of neutral and cationic complexes with the same coordination mode, may also help in tuning the redox characteristics of the complexes formed.

## Experimental Section

The synthesis of $pyr_2en$, $Rpyr_2en$, and $R(SO_3–sal)_2en$ was previously reported.[12,16]

### Synthesis of Complexes

**Crystals of $Ni(pyr_2en)\cdot 3H_2O$ (1):** From the filtrate solution of the reaction mixture used in the preparation of complex **6** orange crystals suitable for X-ray diffraction studies were obtained after six weeks.

**$Cu(pyr_2en)$ (2):** The Schiff base $pyr_2en$ (0.05 g, 0.2 mmol) was dissolved in water (25 mL) and the pH was adjusted to 7 by addition of KOH (3 M). Cupric acetate (0.03 g, 0.1 mmol) was added and the mixture was heated to 50 °C for an hour. A dark pink solid precipitated, which was collected by filtration and washed with water, ethanol, and diethyl ether, and dried under vacuum. Yield: 0.063 g, 68%. $C_{18}H_{20}N_4O_4Cu\cdot 2.3H_2O$ (461.36) {$[Cu(pyr_2en)]\cdot 2.3H_2O$}: calcd. C 46.86, H 5.37, N 12.14; found C 46.9, H 5.5, N 12.0.

**$Cu(Rpyr_2en)$ (3):** The procedure was similar to the one used for **2**. A blue solid was obtained. Yield: 0.043 g, 45%. $C_{18}H_{24}N_4O_4Cu\cdot 2.7H_2O$ (472.60) {$[Cu(Rpyr_2en)]\cdot 2.7H_2O$}: calcd. C 45.75, H 6.27, N 11.86; found C 45.8, H 6.3, N 11.7.

**$Cu\{R(SO_3–sal)_2en\}$ (4):** The procedure was similar to the one used for complex **2**. A green solid was obtained. Yield: 0.053 g, 50.0%. $C_{16}H_{18}N_2O_8S_2Cu\cdot 2H_2O$ (531.03), {$[Cu\{R(SO_3–sal)_2en\}]\cdot 2H_2O$}: calcd. C 36.26, H 4.18, N 5.29, S 12.10; found C 36.2, H 4.5, N 5.1, S 12.5.

**$Ni(pyr_2en)$ (5):** $Pyr_2en$ (0.5 g, 1.4 mmol) was dissolved in methanol (25 mL) containing a few drops of a KOH solution. $Ni(CH_3COO)_2\cdot 4H_2O$ (0.35 g, 1.4 mmol) dissolved in methanol/water (1:1, 25 mL) was slowly added and the mixture became orange. The pH was adjusted to 7 by the addition of methanolic HCl. An orange solid precipitated and was collected by filtration and washed with water, methanol, and diethyl ether, and dried under vacuum. Yield: 0.53 g, 85%. $C_{18}H_{20}N_4O_4Ni\cdot 1.7H_2O$ (445.70) {$[Ni(pyr_2en)]\cdot 1.7H_2O$}: calcd. C 48.51, H 5.29, N 12.57; found C 48.5, H 5.6, N 12.3. $^1H$ NMR [300 MHz, $(CD_3)_2SO$, 297 K]: $\delta$ = 8.23 (s, 2 H, CH=N), 7.47 (s, 2 H, $CH_{arom}$), 4.50 (s, 4 H, $CH_2CH_2$), 3.56 (s, 4 H, $CH_2OH$) and 2.51 (s, 6 H, $CH_3$) ppm. ESI-MS ($H_2O$): $m/z$ = 415.2 $[M + 1]^+$.

**$Ni(Rpyr_2en)$ (6):** The procedure was similar to the one used for **5**. A pink complex was obtained. Yield: 0.47 g, 72%. $C_{18}H_{24}N_4O_4Ni\cdot 2.4H_2O$ (462.34), {$[Ni(Rpyr_2en)]\cdot 2.4H_2O$}: calcd. C 46.76, H 6.28, N 12.12; found C 47.0, H 6.8, N 11.8. $^1H$ NMR [300 MHz, $(CD_3)_2SO$, 297 K]: $\delta$ = 6.97 (s, 2 H, $CH_{arom}$), 4.92 (s, 4 H, $CH_2OH$), 4.24 (s, 4 H, $CH_2NH$), 3.40 (s, 4 H, $CH_2$ $CH_2$), 2.75 (s, 6 H, $CH_3$) ppm. ESI-MS ($H_2O$): $m/z$ = 419.2 $[M + 1]^+$.

**$Ni[(SO_3–sal)_2en]$ (7):** The procedure was similar to the one used for the preparation of **5**. An orange solid was obtained. Yield: 0.35 g, 82%. $C_{16}H_{12}N_2O_8S_2NiK_2\cdot 3.8H_2O$ (629.75) {$K_2\{Ni[(SO_3–sal)_2en]\cdot 3.8H_2O$} calcd. C 30.52, H 3.14, N 4.45, S 10.18; found C 30.7, H 2.5, N 5.2, S 8.7. $^1H$ NMR [300 MHz, $D_2O$, 297 K]: $\delta$ = 7.97 (s, 2

  

H, CH=N), 7.74 (s, 2 H, $CH_{arom}$), 7.55 (d, 2 H, $CH_{arom}$), 6.87 (d, 2 H, $CH_{arom}$), 3.45 (s, 4 H, $CH_2CH_2$).

**Ni[R(SO$_3$–sal)$_2$en] (8):** The procedure was similar to the one used for the preparation of **5**. Since there was no precipitation at pH 7 the solution was evaporated to dryness. Methanol was added to the residue, which did not dissolve everything. The solid was filtered, washed with methanol and diethyl ether, and dried under vacuum. After a few hours the grey solid obtained turned soft pink and after a week brown. Yield: 0.52 g, 62.0%. $C_{16}H_{16}N_2O_8S_2NiK_2{\cdot}8.5H_2O$ (718.45) {$K_2${Ni[R(SO$_3$–sal)$_2$en]·8.5H$_2$O} calcd. C 26.75, H 4.63, N 3.90, S 8.92; found C 27.1, H 4.0, N 4.0, S 7.2. ESI-MS ($H_2O$): $m/z$ = 565.0 $[M + 2K + 1]^+$ and 603.0 $[M + 3K]^+$.

**Physical and Spectroscopic Studies:** Infrared spectra were recorded with a BioRad FTS 3000 MX FTIR spectrometer. UV/Visible spectra were recorded either with a Hitachi U-2000, a Perkin–Elmer Lambda 9 UV/Vis/NIR, or an HP 8452A diode array spectrophotometer. The EPR spectra were recorded with a Bruker ESP 300E X-band spectrometer. $^1$H NMR spectra were recorded with a Varian Unity 300 spectrometer at probe temperature.

**X-ray Crystal Structure Determination:** Three-dimensional X-ray data were collected with a Bruker SMART 1000 CCD diffractometer by the $\varphi$-$\omega$ scan method. Data was collected at room temperature. Reflections were measured from a hemisphere of data collected from frames each covering 0.3° in $\omega$. Of the 12502 reflections measured, all of which were corrected for Lorentz and polarization effects, and for absorption by semi-empirical methods based on symmetry-equivalent and repeated reflections, 1941 independent reflections exceeded the significance level $|F|/\sigma(|F|) > 4.0$. Because of the crystal nature (possibly pseudo-merohedrally twined emulating a metrically orthorhombic cell) and diffraction capabilities, some discrepant reflections were suppressed. Complex scattering factors were taken from the program package SHELXTL.[39] The structures were solved by direct methods and refined by full-matrix least-squares methods on $F^2$. The hydrogen atoms were included in calculated positions and refined by using a riding model, except the hydrogen atoms from the water molecules. Hydrogen atoms H(11W) and H(21W) of one water molecule were located from a difference electron density map and fixed to 0.97 Å from the corresponding heteroatom. Hydrogen atoms of the other two water molecules were left to refine freely. Refinement converged with allowance for thermal anisotropy of all non-hydrogen atoms. Minimum and maximum final electron densities are: –0.586 and 0.758 e Å$^{-3}$. Crystal data and details on data collection and refinement are summarized in Table 5.

Table 5. Crystal data collection and refinement.

| | **1** |
|---|---|
| Formula | $C_{18}H_{26}N_4O_7Ni$ |
| $M_r$ [g mol$^{-1}$] | 469.14 |
| Crystal system | monoclinic |
| Space group | $P2_1/c$ |
| $T$ [K] | 298(2) |
| $a$ [Å] | 8.268(2) |
| $b$ [Å] | 12.637(3) |
| $c$ [Å] | 19.634(5) |
| $\alpha$ [°] | 90 |
| $\beta$ [°] | 90.492(5) |
| $\gamma$ [°] | 90 |
| $V$ [Å] | 2051.3(9) |
| $F$(000) | 984 |
| $Z$ | 4 |
| $D_{calcd.}$ [g cm$^{-3}$] | 1.519 |
| $\mu$ [mm$^{-1}$] | 0.994 |
| $R_{int}$ | 0.1304 |
| No. of measured reflections | 12052 |
| No. of observed reflections | 1941 |
| Data / restraints / parameters | 4705 / 5 / 292 |
| Goodness-of-fit on $F^2$ | 0.938 |
| $R_1$[a] | 0.0953 |
| $wR_2$[b] (all data) | 0.2813 |

[a] $R_1 = \Sigma||F_o| - |F_c|| / \Sigma|F_o|$. [b] $wR_2 = \{\Sigma[w(|F_o|^2 - |F_c|^2)^2]| / \Sigma[w(F_o^4)]\}^{1/2}$.

CCDC-287242 contains the supplementary crystallographic data for this paper. These data can be obtained free of charge from The Cambridge Crystallographic Data Centre via www.ccdc.cam.ac.uk/data_request/cif.

**Solution Studies:** All solutions were manipulated in an inert atmosphere (high purity nitrogen or purified argon). The stock solution of $Cu^{II}$ was prepared and standardized as described earlier.[40] The $Ni^{II}$ stock solution was prepared by dissolving $NiCl_2$ of puriss quality in HCl solution. The $Ni^{II}$ content was determined by complexometry with EDTA, and the free acid content was measured pH-metrically. The ionic strength was adjusted to 0.2 mol dm$^{-3}$ with KCl. For pH-potentiometric measurements the temperature was 25.0 ± 0.1 °C, and for Vis spectra 25.0 ± 0.3 °C with circulating water.

**pH Measurements**

**Spectroscopic Measurements:** For the preparation of the solutions and pH calibrations we used a special glass vessel with a double wall, with entries for the combined electrode (Radiometer "Red Rod" pHC2015–8), thermometer, nitrogen, and reagents (e.g. base). A computerized system developed locally was used to control the titration conditions for pH calibrations. The emf measurements were performed with a Denver Model 15 pH meter.

**pH-Potentiometric Titrations:** Stability constants were determined from pH-metric titrations of 25 mL samples. The ligand concentrations were in the range 0.001–0.004 mol dm$^{-3}$ and the metal ion to ligand molar ratio was varied from 1 to 4 (up to 10 for the Ni–Rpyr$_2$en system). Titrations were normally made from pH 2.0 up to 11.7, but some titration curves started at 1.7, with a KOH solution of known concentration (ca. 0.2 mol dm$^{-3}$) under a purified argon atmosphere. The reproducibility of titration points included in the evaluation was within 0.005 pH units over the whole pH range. For the $Cu^{II}$– and $Ni^{II}$–Rpyr$_2$en systems 5 and 7 titration curves were measured, respectively.

The pH was measured with an Orion 710A precision digital pH meter equipped with an Orion Ross 8103BN type combined glass electrode, calibrated for hydrogen ion concentration as described earlier.[41] The ionic product of water was p$K_w$ = 13.76. The concentration stability constants $\beta_{pqr} = [M_pL_qH_r]/[M]^p[L]^q[H]^r$ were calculated with the aid of the PSEQUAD computer program.[31] When referring to stoichiometries of complexes present in solution the normal $M_pL_qH_r$ notation is used, where L = Rpyr$_2$en$^{2-}$.

**Spectroscopic Measurements:** Visible absorption spectra were measured using cells with 0.1, 1, or 3 cm path lengths. The spectral range covered was normally 300–900 nm, and in some cases 350–1100 nm. For the $Cu^{II}$–Rpyr$_2$en system the EPR (at 77 K) and Vis spectra were recorded varying the pH and using a ligand to metal ratio of approximately 1 and $C_{Cu} \approx 5$ mmol dm$^{-3}$. To obtain data for the low pH range individual samples containing the same metal ion concentration and L/M ratio were also prepared by adding different amounts of HCl. A calibration curve ($E_{measured}$ versus p[H$^+$]) was measured to determine the system response to the [H$^+$] of the samples. The standards were prepared by mixing various accurately

  

known volumes of HCl of known concentration (ca. 0.1 mol dm$^{-3}$) with water. The Vis ($300 < \lambda < 900$ nm) and room temperature EPR spectra of these samples were recorded and used for the determination of the speciation model at low pH, namely the $\log\beta$ of $CuLH_2$ with the PSEQUAD program.[31]

For the $Ni^{2+}$–$Rpyr_2en$ system the spectral range covered was 190–820 nm (for the quantitative evaluation only the 390–820 nm range was used). The absorption spectra were recorded at L/M ratios of 1 and 4 (the total concentrations of the $Ni^{II}$ [$C_M$] were 0.004 and 0.002 mol dm$^{-3}$, respectively). All other experimental conditions were as described for the pH-potentiometric titrations. For the solutions with a L/M ratio of 1 ($C_{Ni}$ = 0.004 mol dm$^{-3}$) precipitation of a pink compound occurred at pH ca. 8.3; this was not observed for solutions with L/M ratios of 4. With the latter solutions, the increasing absorbance of the baseline above pH ca. 9.2 suggested the presence of small amounts of precipitate. In order to confirm the octahedral geometry of the complexes Vis spectra with a L/M ratio of 1 and $C_{Ni}$ = 0.003 mol dm$^{-3}$ were measured at several pH values (3.0–7.7) in the 350–1100 nm range.

In the absence of ethylene glycol a relatively broad background was present in most of the frozen solution EPR spectra; therefore most spectra were run with solutions containing 5% of ethylene glycol.

For the $^1$H NMR measurements, solutions containing $Ni^{II}$ and $Rpyr_2en$ with a L/M ratio of 1 (5 mmol dm$^{-3}$) and 4 (16:4 mmol dm$^{-3}$) were prepared in $D_2O$ (DSS, sodium 3-trimethylsilyl-[$D_4$]propionate, as internal reference), and the pD was adjusted with DCl or $CO_2$ free KOD, using a Crison micropH 2002 instrument fitted with a combined Mettler Toledo U402-M3 S7/200 microelectrode. The microelectrode was previously calibrated with standard buffered aqueous solutions and –log[$D^+$] was measured directly in the NMR tubes. The final values of pD were determined from pD = pH* + 0.40, where pH* corresponds to the reading from the pH meter previously calibrated with two aqueous buffers at pH 4 and 7.

Mass spectrometer experiments were performed with a LCQ Duo (Finnigan, San Jose, CA, USA) ion trap mass spectrometer equipped with an electrospray ion source, operated in the positive mode and maintained at 4.5 kV. The temperature of the heated capillary was set to 200 °C. The flow rate of the electrospray solution was 5 μL min$^{-1}$. Other parameters, including capillary voltage, lens, and octapole voltages and sheath gas flow rate were optimized for maximum abundance of the ions of interest.

The ESI mass spectra measurements were done with solutions of nickel complexes **5**–**8** ($1 \times 10^{-4}$ mol dm$^{-3}$) and of solutions containing $Ni^{II}$ and $Rpyr_2en$ with a L/M ratio of 1 (1 mmol dm$^{-3}$) and 4 (4:1 mmol dm$^{-3}$). All solutions were prepared with deionized water.

**Supporting Information** (see also the footnote on the first page of this article): **ESI-1** Crystalline packing in complex Ni(pyr$_2$en)·3H$_2$O (**1**). **ESI-2** EPR spectra of complex Cu[R-(SO$_3$–sal)$_2$en] (**4**) and $[Cu(OH_2)_6]^{2+}$ in $H_2O$. **ESI-3** Visible spectra for the $Ni^{II}$–$Rpyr_2en$ system with L/M = 1 and 4.

## Acknowledgments

The authors thank Dr Maria da Conceição Oliveira for her help with the ESI mass spectra, Fundação para a Ciência e a Tecnologia (FCT), POCTI (POCTI/QUI/56949/2004 and POCTI/QUI/55985/2004), the Hungarian National Research Fund (OTKA T31896/2000), the Hungarian Academy of Sciences, the bilateral Portugal–Hungary Cooperation Program, the bilateral Acção Integrada Luso-Espanhola E-56/05, and COST D29 Action (D29/0016/04: "Novel sustainable metal-catalysed oxidations with $H_2O_2$ and $O_2$") for financial support.

[1] P. G. Cozzi, *Chem. Soc. Rev.* **2004**, *33*, 410–421.
[2] J. F. Larrow, E. N. Jacobsen, *Top. Organomet. Chem.* **2004**, *6*, 123–152.
[3] T. Achard, Y. N. Belokon, J. A. Fuentes, M. North, T. Parsons, *Tetrahedron* **2004**, *60*, 5919–5930.
[4] E. N. Jacobsen, *Acc. Chem. Res.* **2000**, *33*, 421–431.
[5] T. Katsuki, *Chem. Soc. Rev.* **2004**, *33*, 437–444.
[6] T. Fukuda, T. Katsuki, *Tetrahedron* **1997**, *53*, 7201–7208.
[7] B. D. Brandes, E. N. Jacobsen, *Tetrahedron Lett.* **1995**, *36*, 5123–5126.
[8] M. Valko, R. Klement, P. Pelikan, R. Boca, L. Dlhán, A. Boettcher, H. Elias, A. Muller, *J. Phys. Chem.* **1995**, *99*, 137–143.
[9] A. Boettcher, H. Elias, E. G. Jaeger, H. Langfelderova, M. Mazur, A. Muller, H. Paulus, P. Pelikan, M. Rudolph, M. Valko, *Inorg. Chem.* **1993**, *32*, 4131–4138.
[10] R. Klement, F. Stock, H. Elias, H. Paulus, P. Pelikan, M. Valko, M. Mazúr, *Polyhedron* **1999**, *18*, 3617–3628.
[11] A. Bottcher, H. Elias, L. Muller, H. Paulus, *Angew. Chem. Int. Ed. Engl.* **1992**, *31*, 623–625.
[12] I. Correia, J. Costa Pessoa, M. T. Duarte, R. T. Henriques, M. F. M. Piedade, L. F. Veiros, T. Jackusch, A. Dornyei, T. Kiss, M. M. C. A. Castro, C. F. G. C. Geraldes, F. Avecilla, *Chem. Eur. J.* **2004**, *10*, 2301–2317.
[13] P. Román, A. Aranzabe, A. Luque, M. Gutierrez-Zorrila, M. Martínez-Ripoll, *J. Chem. Soc., Dalton Trans.* **1995**, 2225–2231.
[14] A. Jancsó, I. Torok, L. Korecz, A. Rockenbauer, T. Gajda, *J. Chem. Soc., Dalton Trans.* **2002**, 2601–2607.
[15] E. M. Case, *Biochem. J.* **1932**, *26*, 753.
[16] I. Correia, J. C. Costa Pessoa, M. T. Duarte, M. F. M. Piedade, T. Jackusch, T. Kiss, M. M. C. A. Castro, C. F. G. C. Geraldes, F. Avecilla, *Eur. J. Inorg. Chem.* **2005**, 732–744.
[17] M. Nakai, M. Obata, F. Sekigushi, M. Kato, M. Shiro, A. Ichimura, I. Kinoshita, M. Mikuriya, T. Inohara, K. Kawabe, H. Sakurai, C. Orvig, S. Yano, *J. Inorg. Biochem.* **2004**, *98*, 105–112.
[18] M. Valko, R. Boca, R. Klement, J. Kozísek, M. Mazur, P. Pelikan, H. Morris, H. Elias, L. Muller, *Polyhedron* **1997**, *16*, 903–908.
[19] D. F. Evans, *J. Chem. Soc.* **1959**, 2003–2005.
[20] E. Sinn, A. B. Blake, W. Haussain, R. Paschke, J. R. Chipperfield, *Inorg. Chem.* **1995**, *34*, 1125–1129.
[21] I. C. Santos, M. Vilas-Boas, M. F. M. Piedade, C. Freire, M. T. Duarte, B. de Castro, *Polyhedron* **2000**, *19*, 655–664.
[22] D. H. Williams, I. Fleming, in: *Spectroscopic Methods in Organic Chemistry*, McGraw-Hill, London **1995**, pp. 42–49.
[23] K. Nakamoto, in: *Infrared and Raman Spectra of Inorganic Compounds* **1997**, pp. 73–271.
[24] R. M. Silverstein, G. C. Bassler, T. C. Morril, in: *Spectrometric Identification of Organic Compounds*, John Wiley & Sons, New York, **1991**, pp. 122–125.
[25] G. Socrates, in: *Infrared and Raman Characteristic Group Frequencies. Tables and Charts*, John Wiley & Sons, Chichester, **2001**, pp. 108–113.
[26] A. K. Rappé, C. J. Casewit, K. S. Colwell, W. A. Goddard III, W. M. Skiff, *J. Am. Chem. Soc.* **1992**, *114*, 10024.
[27] A. R. Amundsen, B. Bosnich, *J. Am. Chem. Soc.* **1977**, *99*, 6730–6739.
[28] P. S. Subramanian, E. Suresh, D. Srinivas, *Inorg. Chem.* **2000**, *39*, 2053–2060.
[29] A. Rockenbauer, L. Korecz, *Appl. Magn. Reson.* **1996**, *10*, 29.
[30] U. Sakaguchi, A. W. Addison, *J. Chem. Soc., Dalton Trans.* **1979**, 600–608.
[31] L. Zekany, I. Nagypal, in: *Computational Methods for the Determination of Stability Constants* (Ed.: D. Leggett), Plenum, New York, **1985**.

  

[32] M. S. El-Ezabi, F. M. Al-Sogais, *Polyhedron* **1982**, *1*, 791–798.
[33] B. N. Figgis, M. A. Hitchman, in: *Ligand Field Theory and its Applications*, Wiley-VCH, New York, **2000**, pp. 294–303.
[34] N. N. Greenwood, A. Earnshaw, in: *Chemistry of the elements*, Pergamon Press, London, **1984**, pp. 1144–1172.
[35] S. V. Zublov, I. I. Seifullina, Z. A. Starikova, A. I. Yanovsky, *Zh. Neorg. Khim.* **1999**, *44*, 35–40.
[36] M. N. Tahir, D. Uelkue, H. Nazir, O. Atakol, *Acta Crystallogr. Sect. C* **1997**, *53*, 181–183.
[37] M. Di Vaira, P. Orioli, *Inorg. Chem.* **1967**, *6*, 490–494.
[38] I. Correia, A. Dornyei, F. Avecilla, T. Kiss, J. C. Costa Pessoa, *Eur. J. Inorg. Chem.* **2006**, 656–662.
[39] G. M. Sheldrick, *SHELXT-97, A program for refining crystal structures* (release 5.1), **1997**.
[40] J. Costa Pessoa, L. F. Vilas Boas, R. D. Gillard, R. Lancashire, *Polyhedron* **1988**, *7*, 1245–1262.
[41] R. D. Gillard, J. Costa Pessoa, T. Gajda, T. Kiss, S. M. Luz, J. J. G. Moura, I. Tomaz, J. P. Telo, I. Török, *J. Chem. Soc., Dalton Trans.* **1998**, 3587–3600.

Received: January 12, 2006
Published Online: May 8, 2006

  